A&A 523, A51 (2010)
DOI: 10.1051/0004-6361/201015008

Astronomy & Astrophysics

Tracing gas accretion in the Galactic center using isotopic ratios⋆

D. Riquelme[1], M. A. Amo-Baladrón[2], J. Martín-Pintado[2], R. Mauersberger[3], S. Martín[4], and L. Bronfman[5]

[1] Instituto de Radioastronomía Milimétrica (IRAM), Av. Divina Pastora 7, Local 20, 18012 Granada, Spain
e-mail: riquelme@iram.es
[2] Centro de Astrobiología (CSIC/INTA), Ctra. de Torrejón a Ajalvir km 4, 28850, Torrejón de Ardoz, Madrid, Spain
[3] Joint ALMA Observatory, Av. Alonso de Córdova 3107, Vitacura, Santiago de Chile, Chile
[4] European Southern Observarory, Av. Alonso de Córdova 3107, Vitacura, Casilla 19001, Santiago, Chile
[5] Departamento de Astronomía, Universidad de Chile, Casilla 36-D, Santiago, Chile

Received 17 May 2010 / Accepted 3 August 2010

ABSTRACT

Aims. We study the $^{12}C/^{13}C$ isotopic ratio in the disk of the central molecular zone and in the halo to trace gas accretion toward the Galactic center region in the Milky Way.
Methods. Using the IRAM 30m telescope, we observed the $J = 1–0$ rotational transition of HCO^+, HCN, HNC, and their ^{13}C isotopic substitutions in order to measure the $^{12}C/^{13}C$ isotopic ratio. We observed 9 positions selected throughout the Galactic center region, including clouds at high latitude, locations where the X1 and X2 orbits associated with the barred potential are expected to intersect, and typical Galactic center molecular clouds.
Results. We find a systematically higher $^{12}C/^{13}C$ isotopic ratio (>40) toward the halo and the X1 orbits than for the Galactic center molecular clouds (20–25). Our results point to molecular gas that has undergone a different degree of nuclear processing than observed in the gas towards the inner Galactic center region.
Conclusions. The high isotopic ratios are consistent with the accretion of the gas from the halo and from the outskirts of the Galactic disk.

Key words. Galaxy: center – ISM: clouds – ISM: molecules

1. Introduction

Many galaxies including our Milky Way contain huge amounts of gas in their central few 100 pc (Mauersberger & Henkel 1993; Morris & Serabyn 1996). This gas can be the fuel reservoir that feeds star formation events, and in many cases, the activity of the central object (Usero et al. 2004; García-Burillo et al. 2005). Both processes can occur in bursts. For example, the central region of our Galaxy, which harbors the nearest massive black hole ($\sim 4.0 \times 10^6\ M_\odot$; Ghez et al. 2005), may have been much more active in the past than it is now (Morris et al. 1999). It is obvious that such a high activity level, even if intermittent, can only be maintained if there is a supply of gas from other regions of the Galaxy, e.g. a disk or halo or from intergalactic space.

Modeling the kinematics of the inner regions of galaxies has been successful in explaining inward motion, matching the observations: Binney et al. (1991) have shown that the large-scale gas kinematics in the Galactic center (GC) can be accounted for by a barred galactic potential. In the dynamical model with a barred potential, there are two major families of stable prograde periodic orbits inside the bar: the X1 orbits parallel to the bar, and the X2 orbits orthogonal to it (Contopoulos & Papayannopoulos 1980). In the outer parts of the bar, gas tends to follow the X1 orbits. Farther inwards, these orbits develop cusps and loops (Maciejewski & Sparke 2000), where matter on self-intersecting orbits gets shocked and falls toward the center, and plunges to orbits of the X2 family (Binney et al. 1991).

Another mechanism for gas accretion toward the central region of galaxies is the disk-halo interaction. A clear example of these interactions has been shown recently by Fukui et al. (2006), who found huge loop structures (known as "giant molecular loops"; GMLs) that connect gas at the Galactic plane with gas at higher latitudes.

However, so far there is no clear observational evidence that gas in the outer disk (in X1 orbits) and/or at high latitudes (in the GMLs) flows toward the central regions. Gas in the GMLs could also be ejected to higher latitudes by winds, originated in past massive star formation events (the GC harbors giant molecular clouds with ongoing massive star formation, e.g. in Sgr B and the 1.3 complex). Observations of gas kinematics tell us what is happening now, but do not allow looking into the past. However, studies of the isotope trace the flow since different regions in a galaxy may have their very characteristic isotopic fingerprints. This approach has the potential to reconstruct the migration history to the central part of the galaxy.

Carbon, nitrogen, and oxygen (CNO) isotopic ratios are diagnostic tools for probing models of Galactic chemical evolution (see e.g. Audouze 1985). In particular, the $^{12}C/^{13}C$ isotopic ratio reflects the history of gas proccesing by stars, because this ratio shows the relative degree of primary to secondary processing in stars. While ^{12}C is predicted to be formed in first-generation, metal-poor massive stars, on rapid timescales, ^{13}C is thought to be produced primarily via CNO processing of ^{12}C seeds from earlier stellar generations, on a slower timescale in low and intermediate-mass stars or novae (Meyer 1994; Wilson & Matteucci 1992; Prantzos et al. 1996). The $^{12}C/^{13}C$ isotopic ratio is one of the best-established in the GC. It presents a clear

⋆ Based on observations carried out with the IRAM 30m telescope. IRAM is supported by INSU/CNRS (France), MPG (Germany), and IGN (Spain).

Table 1. Galactic and equatorial coordinates of the emission-free reference positions.

Galactic coordinates		Equatorial coordinates	
l [°]	b [°]	α_{J2000}	δ_{J2000}
5.75	1.0	17:54:56.6	−23:29:13
4.5	−1.29	18:00:57.3	−25:43:12
356.375	1.5	17:30:48.0	−31:11:48
359.75	−0.25	17:46:00.1	−29:16:47
1.0	−1.0	17:51:52.9	−28:35:41
0.65	0.2	17:46:23.0	−28:16:37

gradient with galactocentric distance (e.g., Wilson 1999), decreasing from 80–90 in the solar neighborhood to 20–25 in the inner Galaxy (toward Sgr A and Sgr B, see e.g., Wannier 1980). However, this ratio is, so far, unknown in the galactic halo and in the X1 orbits.

In this paper we present observations of the $J = 1–0$ rotational transition of HCO^+, $H^{13}CO^+$, HCN, $H^{13}CN$, HNC, and $HN^{13}C$ to derive the $^{12}C/^{13}C$ isotopic ratio toward the gas in the halo, the disk, and for the kinematic components associated with the X1 and X2 orbits in the nucleus of our Galaxy. We found very different $^{12}C/^{13}C$ isotopic ratios in the X1 orbits and in the halo from those in the disk and in the X2 orbits. Our findings are consistent with the scenario of less processed gas in the halo and in the X1 orbits, supporting the idea of gas flowing toward the nucleus of the Milky Way.

2. Observations

Observations were carried out with the IRAM-30m telescope at Pico Veleta (Spain) in June and December 2009. We used the E090 band of the new EMIR receiver, which provide a bandwidth of ~8 GHz (from 83.7 to 91.1 GHz) simultaneously in both polarizations. For the backend, we used the WILMA autocorrelator, providing a resolution of 2 MHz or 6.8 km s^{-1}. Observations were performed in position-switching mode where the reference off-positions were checked to be free of emission. Table 1 lists the emission-free positions. The pointing was checked every 2 h against the source 1757-240 providing an accuracy better than 5″. Data were calibrated using the standard dual load system. In this work, we use the antenna temperature scale T_A^*. Main beam temperatures, T_{MB}, can be obtained using $T_{MB} = F_{eff}/B_{eff} \times T_A^*$, where the forward efficiency is $F_{eff} = 95\%$ and the main-beam efficiency is $B_{eff} = 81\%$ at 86 GHz. All positions were observed for no less than 30 min providing an rms noise antenna temperature of about 6 mK in the weakest lines (e.g. $H^{13}CO^+$).

We observed the nine positions shown in Table 2 displayed on the large-scale map of the HCO^+ emission shown in Fig. 1. Five of the observed positions are located in the GMLs (halo in Tables 2, 3, and Fig. 1). Three of them are located at the foot points and two at the top of the loops. Two positions are in the disk toward the locations of the expected interactions between the X1 and X2 orbits (Disks X1 and X2 in Tables 2, 3, and Fig. 1). A pair of positions toward the Galactic plane (Disk in Tables 2, 3, and Fig. 1) were used as reference measurements. The positions at the foot points of the GMLs were selected from the intensity peaks of the SiO maps of Riquelme et al. (2010) and from previous results from higher angular resolution mapping with the Mopra-22 m telescope (Riquelme et al., in prep.). The Fukui et al. (2006) maps of the GMLs were used to select the position at the top of the loop. The positions in the 1.°3 and in Sgr C complexes correspond to the locations where interactions between the X1 and X2 orbits are expected (see, Binney et al. 1991; Stark et al. 2004). The CO and SiO(2−1) maps of these regions (Tanaka et al. 2007; Amo-Baladrón et al., in prep.) were used for final selection of the positions. The control points in the disk are located in Sgr B2 and in the $l = 5.°7$ complex selected from Martín et al. (2008) and Fukui et al. (2006), respectively.

3. Results

Figure 1 shows the spectra taken in all the observed positions in the $J = 1 \rightarrow 0$ transition of the main isotope of HCO^+, HCN and HNC and their ^{13}C isotopologues. All the species have been clearly detected in all our sources, except $HN^{13}C$, with tentative detections in "Halo 1" and "Halo 3", and a nondetection in "Halo 2".

Table 3 shows the integrated line-intensity ratios between the different isotopologues derived for all positions and velocity components. To distinguish between the different kinematical components, the line intensity ratios were obtained by integrating the line profiles in the velocity ranges given in Table 3. We derived line-intensity ratios from three different species, obtained the highest values from HCO^+.

4. The $^{12}C/^{13}C$ isotopic ratios

The isotopologues that we observed in this work have very similar rotational constants and Einstein coefficients, therefore the beam size is very similar. For optically thin emission, one would expect that line intensity ratios would be directly converted into column density ratios, i.e., $\int T_{H^{12}CO^+} dv / \int T_{H^{13}CO^+} dv = N(H^{12}CO^+)/N(H^{13}CO^+) = [H^{12}CO^+]/[H^{13}CO^+]$.

In general, the molecular isotopologue ratios (see Table 3) do not translate directly into $^{12}C/^{13}C$ isotopic ratios. Opacity, chemical fractionation, and selective photodissociation effects must be considered to derive the isotopic ratios from molecular line-intensity ratios. In the following, we discuss the importance of these effects on the $^{12}C/^{13}C$ isotopic ratios that we derive from our integrated intensity ratio of the isotopologues.

4.1. Opacity effects, isotopic fractionation, and selective photodissociation

In our case, it is impossible to estimate the line optical depth from the emission of just one single transition. Since optical depth effects will saturate the emission from the most abundant isotopologue, our derived molecular isotopic ratios must be considered to be lower limits to the actual $^{12}C/^{13}C$ isotopic ratios. In almost all cases, the $HCO^+/H^{13}CO^+$ intensity ratios or their limits are higher than those derived from the HCN and HNC isotopomers. This may be interpreted as HCO^+ being the least optically thick among the three molecular line emissions used in this work. Therefore, $HCO^+/H^{13}CO^+$ intensity ratios give the most stringent limits to the $^{12}C/^{13}C$ isotopic ratios. We still cannot exclude that HCO^+ is also affected by opacity effects, which means that $^{12}C/^{13}C$ isotopic ratios are even higher than inferred from the $HCO^+/H^{13}CO^+$ intensity ratios. In the following, we therefore only consider the isotopologue ratios derived from HCO^+.

Another important effect may be chemical fractionation (Wilson 1999, and references therein). Langer et al. (1984) studied the fractionation of carbon and oxygen isotopes with a time-dependent chemical model. Their model considers a cloud lifetime of 10^8 years, temperatures from 6 to 80 K, H_2 densities

Table 2. Observed positions.

Associated object	Galactic coordinates l [°]	b [°]	Equatorial coordinates α_{J2000}	δ_{J2000}	This work
M+5.3 − 0.3	5.45	−0.324	$17^h59^m17.8^s$	−24°24′38″	Halo 1
M−3.8 + 0.9	356.206	0.83	$17^h32^m59.8^s$	−31°42′17″	Halo 2
M−3.8 + 0.9	356.179	0.925	$17^h32^m33.2^s$	−31°40′31″	Halo 3
Top Loop	4.75	−0.8	$17^h59^m34.9^s$	−25°15′16″	Halo 4
Top Loop	356.549	1.339	$17^h31^m52.5^s$	−31°08′19″	Halo 5
1.3 complex	1.28	+0.07	$17^h48^m21.9^s$	−27°48′19″	Disk X1-1, Disk X2-1
Sgr C	359.446	−0.124	$17^h44^m46.9^s$	−29°28′25″	Disk X1-2, Disk X2-2
Galactic plane at $l \sim 5.'7$	5.75	0.25	$17^h57^m46.5^s$	−23°51′51″	Disk 1
Sgr B2	0.6932	−0.026	$17^h47^m21.9^s$	−28°21′27″	Disk 2

Table 3. Intensity ratios from the observed ^{12}C and ^{13}C isotopomers.

Source	Velocity component LSR [km s^{-1}]	Velocity range [km s^{-1}]	$HCO^+/H^{13}CO^+$ ratio of $\int T_A^* dv$	$HCN/H^{13}CN$ ratio of $\int T_A^* dv$	$HNC/HN^{13}C$ ratio of $\int T_A^* dv$
Halo 1	100	[50, 190]	45.5± 5.4	13.5±0.2	≥ 25.6
	87	[50, 97]	≥73.9	25.8±2.0	≥7.5
	117	[97, 135]	32 ± 3.7	11.3±0.1	≥37.5
	144	[135, 190]	39.1±24.7	16.7±1.8	≥2.7
Halo 2	−62	[−115, −20]	73.1±36.5	14.6 ±1.0	≥15.4
	left wing	[−115, −70]	≥34.4	21.2 ±3.3	≥8
	right wing	[−70, −20]	53.2±26.1	11.6 ±0.9	≥13.6
Halo 3	−60	[−120, −30]	38 ±5.0	13 ±0.3	≥40.1
	left wing	[−120, −80]	54.2 ±37.7	19.2 ±1.9	≥10.4
	central peak	[−80, −30]	35.7 ±4.0	12 ±0.2	48.3 ± 21.8
Halo 4	200	[150, 250]	28.3 ±5.4	11.8 ±0.9	14.9 ±3.1
	peak	[150, 210]	29.2 ±7.5	11.7 ±0.8	17.9 ±3.9
	right wing	[210, 250]	≥10.6	12.4 ±4.0	7.1 ±3.4
Halo 5	−50	[−100, −40]	13.8 ±5.0	6.9 ±0.3	22.8 ±12
Disk X1-1	180	[140, 230]	56 ± 6.4	10.8 ±0.1	25.5 ± 7.5
	left wing	[140, 180]	57.2 ± 7.5	11.6 ±0.1	≥8
	right wing	[180, 230]	54.4 ± 11	9.9 ±0.2	15.7 ± 4.4
Disk X2-1	95	[50, 140]	29 ± 1.6	12.1 ± 0.2	22.1 ± 2.7
	left wing	[50, 92]	32.4 ± 3.7	13.9 ± 0.4	22.8 ± 4.0
	right wing	[92, 140]	27.3 ± 1.7	11.3 ± 0.2	21.7 ± 8.6
Disk X1-2	67	[0, 100]	42.1± 8.6	9.4 ± 0.1	9.9 ± 1.3
Disk X2-2	−43	[−80, −20]	21.7 ±1.9	6.6 ±0.1	13.1 ±1.0
Disk 1	66	[35, 105]	14.0 ±2.8	13.1 ± 1.0	15.8 ± 3.6
	central peak	[35, 70]	16.4 ±4.6	23.1 ± 3.8	≥11.4
	right wing	[70, 105]	11.6 ±3.4	7.8 ± 0.7	11.7 ± 2.7
Disk 2	left wing	[0, 43]	≥29.1	9.1 ± 0.2	≥21.9
	55	[43, 97]	4.1 ± 0.1	3.5 ± 0.1	3.7 ± 0.1
	right wing	[97, 135]	16.1 ± 2.3	13.8 ± 1.3	≥2.6

from 5×10^2 to 1×10^5 cm^{-3}, and a wide range of metal abundances. Fractionation in HCO^+ has also been studied by Woods & Willacy (2009) for protoplanetary disks, which can have a greater impact on the $^{12}C/^{13}C$ ratio, but with temperatures and densities different from the GC. Langer et al. (1984) found that the behavior of the carbon isotope ratios can be split into three groups: CO, HCO^+, and "carbon-isotope pool" (which includes the remaining carbon species, such as C^+, H_2CO, CS, etc). They found that the ^{13}C is enhanced in the CO (specially at low temperature, low density, and high metal abundance), that the ^{12}C is enhanced in the "carbon isotope pool" group, and that the HCO^+ could present both fractionation effects, depending on the physical condition. The behavior of HCO^+ is related to the formation of this molecule from both CO and from the "carbon pool isotopes". The formation of HCO^+ has been explained by the ion-molecule chemistry (Wilson et al. 2009), where the reaction

$$H_3^+ + CO \leftrightarrow HCO^+ + H_2 \quad (1)$$

likely leads the production of HCO^+. $H^{13}CO^+$ is more tightly bound than HCO^+ by 0.8 meV (9 K). The reactions that have the potential to produce isotopic fractionation occurs by proton-switching reactions between formyl ions and carbon monoxide by (Langer et al. 1978, 1984)

$$HCO^+ + ^{13}CO \leftrightarrow H^{13}CO^+ + ^{12}CO + 9\ K. \quad (2)$$

As shown in Fig. 1 of Langer et al. (1984), the isotopic ratio derived from HCO^+ presents only moderate fractionation. The $H^{12}CO^+/H^{13}CO^+$ ratio is slightly enhanced at low density and moderate temperature, and decreases at low temperatures and certain densities ($n(H_2) < 10^3$ and $n(H_2) > 10^{4.5}$). In this model, Langer et al. (1984) considered the formation paths of HCO^+ shown in the Table 2 of Graedel et al. (1982). Hüttemeister et al. (1998) and Rodríguez-Fernández et al. (2002) find that the gas in the GC has temperatures ranging from 20 to 200 K. For this temperature range, the predicted fractionation of HCO^+ is negligible so the fractionation of ^{13}CO cannot occur. In the worst case, the isotopic ratio throughout the GC should not increase

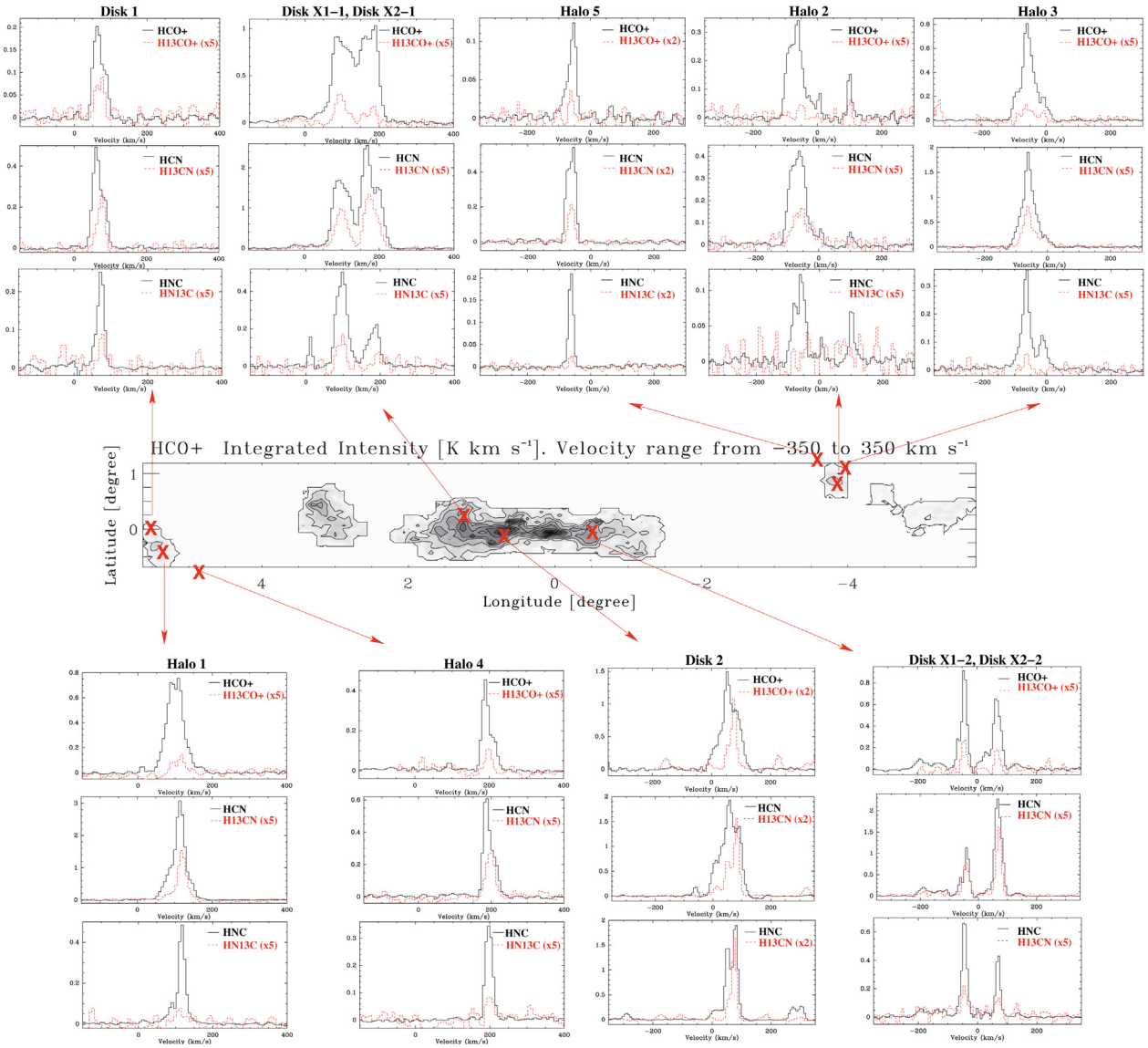

Fig. 1. Spectra toward selected positions in the GC in HCO^+, $H^{13}CO^+$, HCN, $H^{13}CN$, HNC, and $HN^{13}C$. The positions are indicated in the HCO^+ integrated intensity map from Riquelme et al. (2010). The main isotope is plotted in black solid line. The ^{13}C isotope is plotted in red dashed line. The ^{13}C substitution is scaled by a factor of 2 or 5 to allow an easy visualization of the spectra. The factor is indicated in each spectrum.

selectively one of the molecular isotopologue against the other by more than 20%.

For molecular clouds affected by UV radiation, selective photodissociation can take place, which would increase the $^{12}C/^{13}C$ isotopic ratio. The more abundant molecules (the main isotopologues) are less affected by photodissociation through self-shielding against UV radiation than the rarer isotopologues. So far, studies of the HCO^+ and its ^{13}C isotopologue in PDRs have not shown any clear evidence of selective photodissociation (Fuente et al. 2003). Milam et al. (2005) conclude that the $^{12}C/^{13}C$ isotopic ratio derived from high-density tracers like CN are very unlikely to be influenced by isotope-selective photodissociation. However the self-shielding and photodissociation of CO (e.g., Bally & Langer 1982; Chu & Watson 1983; Glassgold et al. 1985) could affect our derived $^{12}C/^{13}C$ ratios through formation of HCO^+ via the reaction in Eq. (1). When modeling this effect, Chu & Watson (1983) concluded that the selective photodissociation will have a negligible impact on the $^{13}CO/^{12}CO$ ratio. Although the local enviroment of the GMLs is so far unknown, there are no signposts of UV radiation. There is only a nearby ultracompact H II region identified at $(l, b) \sim (356.^{\circ}25, 0.^{\circ}7)$, but its radial velocity of ~120 km s^{-1}suggests that it is not associated with the foot points of the GMLs (Torii et al. 2010), making it very unlikely that there is any effect on our derived isotopic ratios by photodissociation. The low $^{13}CO/^{12}CO$ ratio observed in the GMLs by Torii et al. (2010) does not confirm that the bulk of the gas is neither self-shielded in ^{12}CO nor photodissociated in ^{13}CO. The low ratios likely comes from optically thick emission in ^{12}CO, suggesting rather high CO column densities. Then the bulk of the gas will not be affected by the rather low fluxes of far UV radiation inferred from the lack of H II regions (Torii et al. 2010) in the area. Under these conditions, it is highly unlikely that the fractionation/self-shielding effect in the $^{13}CO/^{12}CO$ could explain the observed high $H^{12}CO^+/H^{13}CO^+$ ratios. We conclude that the line-intensity ratios derived from our data correspond to a lower limit to the actual $^{12}C/^{13}C$ isotopic ratio.

We derived $H^{12}CO^+/H^{13}CO^+$ intensity ratios from 4 to >74. The lowest value of 4 is found toward the source Disk 2 in the position of Sgr B2, where one would expect a value of ~25. Such a

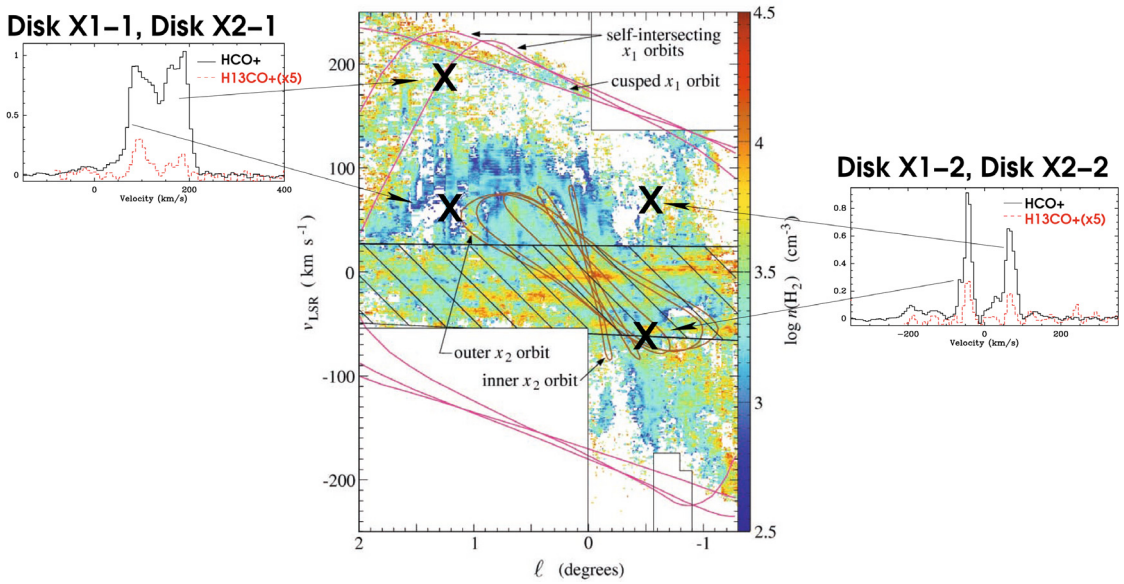

Fig. 2. Spectra toward the X1 and X2 orbits in HCO^+ and $H^{13}CO^+$ (scaled by a factor of 5). *Left*: spectra toward the 1.3 complex. *Center*: l-v diagram showing the X1 and X2 orbits superimposed (Stark et al. 2004). *Right*: spectra toward Sgr C region.

low measured value indicates that HCO^+ is optically thick. From the results in Table 3, we find a systematic trend in the isotopologue ratios with the highest values, >74, found toward Halo 1 and Halo 2. Also Halo 3 and Disk X1-1 and Disk X1-2 show high values of >42.

5. Discussion

It is remarkable that there is a systematic trend by the $^{12}C/^{13}C$ isotopic ratio, found toward the halo and in the disk for the kinematic components associated with the X1 orbits, to be systematically higher by a factor of at least 2 than the standard value in the GC of ∼25. This suggests that there is less processed material in the halo and in the X1 orbits than in the X2 orbits and the reference GC positions in the disk.

Surprisingly, the isotopic ratios measured in the Halo 4 and Halo 5 positions at the top of the GMLs show a lower $^{12}C/^{13}C$ isotopic ratio than in the other halo positions, which are closer to the "standard" values of the disk. From our data, it is still not clear if this low isotopic ratio is comes from opacity effects in the main isotope or from a mixture with more processed gas from stellar nucleosynthesis in the GC region, likely ejected to high latitudes from the disk.

5.1. History of the chemical evolution of the molecular gas in the Galactic center

The lower limits to the $^{12}C/^{13}C$ isotopic abundance ratios derived from our HCO^+ data toward the "typical" GC molecular clouds (Disk 1, Disk 2, Disk X2-1, Disk X2-2) range between 4 to 32, with an average value of 20. These results agree with the values found in the literature for the GC (20–25, Wilson 1999) and with the average value derived by Riquelme et al. (2010) of 19.8 (from the $HCO^+/H^{13}CO^+$ integrated intensity ratio throughout the GC region), showing a considerable nuclear processing. In contrast, we have found much higher limits to the isotopic ratios toward the locations where gas in the inner disk[1] is expected to be interacting with gas in the halo and in the disk. Indeed, the gas in the X1 orbits has a different nature than in the X2 orbits, as clearly reflected by their different isotopic ratios of ∼55 and ∼21−30, respectively. Furthermore, in the halo, the interaction occurs when the gas in the top of the loops flows toward the foot points of the GMLs. In both cases, the isotopic ratio reflects a different nature of the gas than in the GC. The $^{12}C/^{13}C$ isotopic ratio of the gas in the halo and in the X1 orbits are in general higher than 40, reaching values over 70 in "Halo 1".

Previous studies show a clear gradient in the $^{12}C/^{13}C$ ratio with galactocentric distance. The ratio changes from a value of about 50 in the inner Galaxy (4 kpc) to nearly 70 in the local ISM, and ∼90 in the solar system, with a value ∼20−25 in the GC (Wilson 1999), which reflects higher nuclear processing toward the inner Galaxy. Studies of the isotopic ratios in the GC (Wannier 1980; Stark 1981; Henkel et al. 1985; Langer & Penzias 1990) have shown that the interstellar gas in the GC is in an advanced state of chemical evolution (which corresponds to an enrichment of ∼3–4 with respect to the local gas). This gradient indicates that the material is flowing to the inner central kiloparsec of the GC from the Galactic halo (in the case of GMLs) and the outskirts of the Galactic disk (in the case of X1-X2 interacting orbits).

5.2. The origin of molecular gas in the GML

Our lower limits to the $^{12}C/^{13}C$ isotopic ratios in the halo sources for the foot points of the GMLs are close to the values measured in the local ISM (69 ± 6, Wilson 1999). Based on energetic and morphological arguments, Fukui et al. (2006) argue that it is impossible that the loop features are created by supershells or supernova explosions. Our data strongly support their claim. If the loop features were formed by supernova or hypernova explosions, the gas at the foot points should have been ejected from the GC to high latitudes, reflecting the isotopic ratio found throughout the GC. It is likely that the gas in the GMLs has been accreted

[1] Throughout this work, all the positions observed and discussed are in the Galactic center region (in the central kpc of the Galaxy). We denote "disk" as the disk in the CMZ, "inner disk" to the allowed velocities in the X2 orbits, and "outer disk" and "outskirts of the disk" as the noncircular motions (X1 orbits).

from high latitudes. However, if the low isotopologue ratio found at the top of the loops is confirmed to be the actual isotopic ratios, this might indicate that some gas in the halo could also have been ejected from the disk.

Magneto-hydrodynamical simulations have been successful in explaining the formation of the loops (Matsumoto et al. 1988; Horiuchi et al. 1988; Fukui et al. 2006; Machida et al. 2009; Takahashi et al. 2009). They claim that the GMLs have been formed as a natural consequence of a differentially rotating magnetized gas disk under a strong gravitational potential (Machida et al. 2009). It is found that the loop efficiently accumulates gas generating a dense layer at the top of the loops. However, our results are not consistent with the magneto-hydrodynamical loop scenario in which the gas in the GML falling to their foot point should share the same isotopic ratios as the gas in the Galactic disk. Morris (2006) also point out that there is too much gas left at the top of the loops if the gas is flowing down along the magnetic field lines. Morris (2006) and Torii et al. (2009) alternatively propose that ambient HI gas may be converted in the GML into H_2 during flotation. It is likely that the loops are surrounded by H I gas. The rising portion of the magnetic loops suffer shocks that compress the relatively rarefied atomic gas in front of it, leading to rapid cooling and, ultimately, to a phase transition from atomic to molecular gas Morris (2006). Therefore the molecular gas that defines the loops is constantly replenished. This scenario also confirms our results, because the gas in the foot point of the loop has not yet been processed by star formation.

5.3. Gas accretion from the outer disk

We have also found high isotopic ratios toward the noncircular components in the nuclear disk, which have been explained in terms of a stellar-bar driven potential (Binney et al. 1991). The 1.°3 complex has been observed and studied by several authors (Tanaka et al. 2007; Oka et al. 2001; Hüttemeister et al. 1998). This molecular complex shows broad velocity widths and a large latitudinal height scale. The molecular emission shows two velocity components, one centered at ∼110 km s^{-1} and the other at ∼190 km s^{-1}, which correspond to our Disk X2-1 and Disk X1-1 sources, respectively. Tanaka et al. (2007) find an enhancement of the CO $J = 3–2$, HCO^+ $J = 1–0$, HCN $J = 1–0$ with respect to the CO $J = 1–0$, and an enhancement in the abundance of SiO in the high-velocity component (>110 km s^{-1}). They also identify several expanding shells that are very prominent at $v_{LSR} < 110$ km s^{-1} associated with recent star formation. They conclude that the two components correspond to different types of gas with different kinematics and physical conditions. Our Disk X1-1 component presents an enhancement of the SiO/^{13}CO intensity ratio of a factor ∼3 (Tanaka et al. 2007) with respect to the lower velocity component (Disk X2-1). Like Hüttemeister et al. (1998), Tanaka et al. (2007) explains the high SiO abundance as a consequence of recent shock activity.

From our measurements of isotopic ratios, we conclude that the gas associated with the lowest velocity component presents a "typical" GC isotopic ratio consistent with previous ideas of chemistry dominated by shocks generated by supernova explosions. It is very unlikely, however, that the higher velocity component, Disk X1-1, could be associated to the supernova scenario, like the Disk X2-1 component does, as also inferred from the high isotopic ratio found toward this source. The most likely scenario is that the high SiO abundance is the result of the shocks generated by the transfer of gas between the X1 and X2 orbits as suggested by the potential bar scenario.

6. Conclusions

We have determined lower limits to the ^{12}C/^{13}C isotopic ratio toward 9 positions in the GC region, both in the disk and in the halo. In contrast to the values found in the disk sources (∼4–30), we found high isotopic ratios toward the locations where the disk-halo (∼>40–>70) and X1-X2 orbit interactions (>42–>56). Our results are consistent with a scenario where gas from the halo is accreted to the disk and with the transfer of gas from the outskirt of the disk to the GC through X1 and X2 orbits as suggested by the potential bar scenario.

Acknowledgements. D.R. and R.M. were supported by DGI grant AYA 2008-06181-C02-02. J.M-P. and S.M. have been partially supported by the Spanish 74 MICINN under grant number ESP2007-65812-C02-01, and by AYA2010-21697-C05-01. L.B. acknowledges support from FONDAP Center for Astrophysics 15010003 and from Center of Excellence in Astrophysics and Associated Technologies (PFB 06).

References

Audouze, J. 1985, in ESO Astroph. Symp., ed. I. J. Danziger, F. Matteucci, & K. Kjar, 21, 373
Bally, J., & Langer, W. D. 1982, ApJ, 255, 143
Binney, J., Gerhard, O. E., Stark, A. A., Bally, J., & Uchida, K. I. 1991, MNRAS, 252, 210
Chu, Y., & Watson, W. D. 1983, ApJ, 267, 151
Contopoulos, G., & Papayannopoulos, T. 1980, A&A, 92, 33
Fuente, A., Rodríguez-Franco, A., García-Burillo, S., Martín-Pintado, J., & Black, J. H. 2003, A&A, 406, 899
Fukui, Y., Yamamoto, H., Fujishita, M., et al. 2006, Sci., 314, 106
García-Burillo, S., Combes, F., Schinnerer, E., Boone, F., & Hunt, L. K. 2005, A&A, 441, 1011
Ghez, A. M., Salim, S., Hornstein, S. D., et al. 2005, ApJ, 620, 744
Glassgold, A. E., Huggins, P. J., & Langer, W. D. 1985, ApJ, 290, 615
Graedel, T. E., Langer, W. D., & Frerking, M. A. 1982, ApJS, 48, 321
Henkel, C., Güsten, R., & Gardner, F. F. 1985, A&A, 143, 148
Horiuchi, T., Matsumoto, R., Hanawa, T., & Shibata, K. 1988, PASJ, 40, 147
Hüttemeister, S., Dahmen, G., Mauersberger, R., et al. 1998, A&A, 334, 646
Langer, W. D., Graedel, T. E., Frerking, M. A., & Armentrout, P. B. 1984, ApJ, 277, 581
Langer, W. D., & Penzias, A. A. 1990, ApJ, 357, 477
Langer, W. D., Wilson, R. W., Henry, P. S., & Guélin, M. 1978, ApJ, 225, L139
Machida, M., Matsumoto, R., Nozawa, S., et al. 2009, PASJ, 61, 411
Maciejewski, W., & Sparke, L. S. 2000, MNRAS, 313, 745
Martín, S., Requena-Torres, M. A., Martín-Pintado, J., & Mauersberger, R. 2008, ApJ, 678, 245
Matsumoto, R., Horiuchi, T., Shibata, K., & Hanawa, T. 1988, PASJ, 40, 171
Mauersberger, R., & Henkel, C. 1993, Rev. Modern Astron., 6, 69
Meyer, B. S. 1994, ARA&A, 32, 153
Milam, S. N., Savage, C., Brewster, M. A., Ziurys, L. M., & Wyckoff, S. 2005, ApJ, 634, 1126
Morris, M. R. 2006, Sci., 314, 70
Morris, M., & Serabyn, E. 1996, ARA&A, 34, 645
Morris, M., Ghez, A. M., & Becklin, E. E. 1999, Adv. in Space Res., 23, 959
Oka, T., Hasegawa, T., Sato, F., et al. 2001, ApJ, 562, 348
Prantzos, N., Aubert, O., & Audouze, J. 1996, A&A, 309, 760
Riquelme, D., Bronfman, L., Mauersberger, R., May, J., & Wilson, L. T. 2010, 115, A&A, accepted [arXiv:1006.3438]
Rodríguez-Fernández, N. J., Martín-Pintado, J., de Vicente, P., & Fuente, A. 2002, Ap&SS, 281, 331
Stark, A. A. 1981, ApJ, 245, 99
Stark, A. A., Martin, C. L., Walsh, W. M., et al. 2004, ApJ, 614, L41
Takahashi, K., Nozawa, S., Matsumoto, R., et al. 2009, PASJ, 61, 957
Tanaka, K., Kamegai, K., Nagai, M., & Oka, T. 2007, PASJ, 59, 323
Torii, K., Kudo, N., Fujishita, M., et al. 2009, PASJ, 62, 1307
Torii, K., Kudo, N., Fujishita, M., et al. 2010, PASJ, 62, 675
Usero, A., García-Burillo, S., Fuente, A., Martín-Pintado, J., & Rodríguez-Fernández, N. J. 2004, A&A, 419, 897
Wannier, P. G. 1980, ARA&A, 18, 399
Wilson, T. L. 1999, Rep. Progr. Phys., 62, 143
Wilson, T. L., & Matteucci, F. 1992, A&A Rev., 4, 1
Wilson, T. L., Rohlfs, K., & Hüttemeister, S. 2009, Tools of Radio Astronomy (Springer-Verlag)
Woods, P. M., & Willacy, K. 2009, ApJ, 693, 1360